ISSN : 0974 - 7532 Volume 7 Issue 10

Research & Reviews in

BioSciences

Regular Paper

RRBS, 7(10), 2013 [383-393]

Holographic interferometry as a reliable tool visualizing an influence of low-energy fields on biological systems

Galina Dovbeshko[1], Nadia Gridina[2], Volodymyr Krasnoholovets[1]*

[1]Institute of Physics, National Academy of Sciences, Prospect Nauky 46, Kyiv UA-03028, (UKRAINE)

[2]Institute of Neurosurgery, Medical Academy of Sciences 32 Manuilsky St., Kyiv UA-04050, (UKRAINE)

E-mail: v_kras@yahoo.com

ABSTRACT

Holographic interferometer technique has been used to demonstrate an influence of weak physical fields on model biological systems, such as aqueous solutions of DNA molecules, bovine and human serum albumine and embrio tissues, and human blood plasma. Two types of low-energy physical fields of different fundamental nature have been applied: a microwave electromagnetic field with frequencies in the range of tens of GHz and the inerton (inertia) field with a frequency of about 8 Hz. Obtained interference patterns demonstrate peculiar changes in the model biological systems – the rearrangement of macromolecules, which possess a long memory of the influence, up to tens of minutes.

KEYWORDS

Holographic interferometry;
Biological molecules;
Microwave radiation;
Inerton field effects.

INTRODUCTION

Holographic interferometry allows one to fix even a very low change of the refraction index of the system studied, which cannot be measured by other precise methods. Indeed, a holographic interferometer IGD-3 designed and produced at the Institute of Physics of Semiconductors of the National Academy of Sciences of Ukraine makes it possible to distinguish changes in the refraction index with accuracy up to $\Delta n = 10^{-6}$.

By using this precision tool, we carried out a number of studies of different systems. We have been interested in how low intensive physical fields affected samples, such as aqueous solutions of DNA molecules, bovine and human serum albumin, embryo tissue and various organs of rats and mice, etc.

The problem of the interaction of low-intensity electromagnetic radiation of high frequency (in the millimetre range) with biological systems still does not attract a wide attention of academic science. However, because of its practical importance for medicine and biology, it has become one of the most important problems for researchers working in these areas[1-6]. Nowadays the number of natural and artificial sources, which generate weak microwave (MW) radiation, is increasing every day, e.g. power MW pulse furnaces, mobile phones, etc. In addition, the weak interactions play a great role in the structure of biological molecules in their functional state[1]. Despite a growth of information on biophysical experiments with MW electromagnetic field effects and their biomedical applications, there exist a number of problems in fundamental interpretation of the data obtained[2-9]. Obviously, it is determined by physical and chemical complexity of the objects and the dif-

Regular Paper

ficulties of the experiments.

Besides, we have investigated an influence of a low intensive inerton field (inertia field) on solutions of biomolecules, which modelled the living organism[10] (see Section 4). The inerton field with a frequency of about 8 Hz was generated by a Teslar chip, which represented a ferromagnetic band folded and connected, so that it formed a Möbius strip[11,12].

In this paper we present the experimental data on changes of physical characteristics of model biological systems affected by MW radiation and the inerton field by using visible refraction.

MATERIALS & METHOD

Experiments were carried out with the use of the holographic interferometer, whose optical scheme is given in Figure 1. Holographic experiments have been carried out with the use of the holographic interferometer IGD-3.

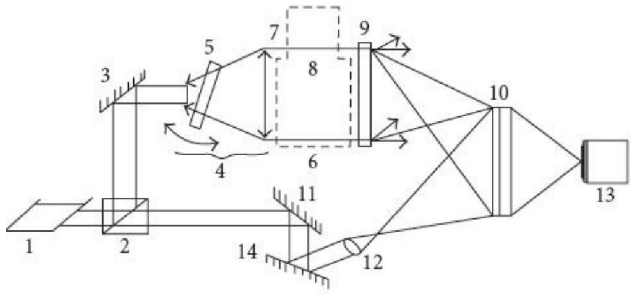

Figure 1 : Experimental holographic set-up: "1" He-Ne laser; "2" beam splitter cube; "3" mirror; "4" collimator; "5" plane parallel plate; "6" quartz flask (cuvette) with solution; "7" one more quartz flask (cuvette) with a solution, or the source of a physical field; "8" filter, which divides two flasks; "9" scattering layer; "10" thermoplastic recording plate; "11" reference beam mirror; "12" reference beam lens; "13" TV camera.

The He-Ne laser "1" radiation (output power 1 mW at $\lambda = 632.8$ nm) is divided by beam splitter cube "2" into two beams: object beam and reference beam. In the object beam there is a mirror "3" and a collimator "4" consisting of negative and positive lenses, which form a parallel beam with 5 cm in diameter. The beam passes through the object under study "6", and then arrives at finely dispersed diffuse scatterer "9". According to Lambert's law, all its points are scattering the light in all directions. Therefore, the light from the whole surface of the scatterer arrives at every point of the light sensitive thermoplastic "10". In the thermoplastic's plane, the object beam together with the reference beam produced by mirror "11" and objective lens "12" form a holographic image of the object under study, in this case the cuvette. The hologram is observed on the monitor screen with camera "14" connected to a computer, which is used for recording and processing of the holograms.

From a special facility a short high voltage was applied to the thermoplastic, which allowed the recording of a hologram formed on the thermoplastic's surface. After that an additional different path of interfering beams is made by changing the inclination of plate "5". After the hologram is registered, a plane-parallel plate "5" is introduced in the object beam, resulting in the appearance of interference patterns on the thermoplastic plate. Pictures of the object and interference patterns are observed by a video camera connected to a computer. With the help of glass plate "5", which introduces phase, the regime of the interference picture can be selected. Thus, at one inclination of the plate "5" the increase of refraction index results in the increase of the interference period, i.e. in the decrease of the number of bands. While at another inclination (with the same sign of n) it leads to the decrease of the interference period and an increase of the number of bands. In our experimental set-up, the plate "5" was positioned in such a way that the increase of the refraction index of the solution in the flask resulted in the decrease of the number of interference bands in the area on the screen which corresponds to the sample. On the other hand, the decrease of the refraction index n (e.g. at the expense of thermal expansion) would cause the increase of the observed number of bands in the area of the sample. In this case, the number of interference bands outside the area of the flask remained unchanged and served for independent control over the object's alterations. If the dielectric characteristics of the object under study are the same before and after MW action, then the interference picture remains unaltered, and interference bands inside and outside the object's profile complement each other. On the contrary, the interference picture within the limits of object's profile changes, in particular, the number of lines and the distance between them changes, if some external factor caused changes of the refraction index of the object.

Changes in the refractive index n of the sample are estimated from the equation $L\Delta n = \lambda \Delta k$,(1) where L

is the thickness of the sample (the aqueous solution studied), Δn is the change in refractive index, λ is the wavelength of the source of light (laser), Δk is the change in the number of interference bands as a result of an external effect.

RESULTS AND DISCUSSION

Microwave radiation

Measurements have been conducted as follows. The cell with 0.9% aqueous solution of NaCl is placed in the interferometer, then the hologram is recorded and the turn of plate (5) introduces interference bands. The same solution combined with bio-additives is filled into a vial. The value and volume of the bio-object(s) have been strictly fixed to determine the percentage of bio-additives. The vial is closed with a filter (Millipore, USA) with hole diameter equal to 0.23 micron. Then the vial is turned upside down and quickly introduced into the cuvette with the filter down. Thus the filter separates two solutions, one of which (top) contains supplements. The height of the column of aqueous solution in the vial is 3 cm. Due to leakage of biological components from the upper to the lower solution the refractive index of the latter changes and the interference pattern is shifted. The shift of interference fringes during a certain time period is recorded visually. In all the experiments conducted the shift is measured for 15 min. (30 seconds after the contact of the two solutions with the filter membrane). The direction of the shift of the interference bands allows us to judge the decrease or increase in optical density of the solution, which points to changes in the refractive index of the solution in the cuvette.

For the irradiation of samples of embryo tissues we used commercial generators (G4-141 and G4-142, Vilnius) that operate with a backward wave tube at the frequency tuned within the range of 37.5 – 78.5 GHz and maximum output power density of 10 mW/cm^2 with frequency stability 5 MHz served as the sources of MW irradiation. To apply the irradiation, a flexible Teflon waveguide with 2.8×5.6 mm^2 cross-section was used. One of its ends was put in the aperture of the generator's metal output waveguide while the free end was lowered into a quartz cuvette ($1 \times 1 \times 4.3$ cm^3) with the studied solution to a depth of 2-3 mm. The exposition was performed at the fixed frequencies selected to achieve maximum effects. Investigations were carried out at the temperature of 20 °C controlled by thermocouple accurate to 0.2 °C.

For the irradiation of samples of blood plasma water solution we used a generator MRT-01 (Kharkiv, Ukraine), which operates in a narrow range of frequencies, 58 to 62 GHz.

Samples of bovine and human serum albumin, and Na-DNA (Servo)

Na-DNA (Servo), bovine and human serum albumin (Reonal), homogenates of embryonic and mature tissues from different organs (kidney, thyroid, gland, spleen and liver) of experimental rats and human blood plasma were used in the experiments. Each time before placing the tubes in a cell we used a new filter.

Because of the small-diameter holes in the separating filter-membrane, 0.23 micron, only molecules and ions can seep through, but not cells. Once the same NaCl solution was in the cell and the vial, no movement of the fringe was observed for at least 15 minutes. Irradiation of the solution in a test vial by MW radiation did not lead to a shift of interference fringes as either.

If we add to the vial with a solution of NaCl, a homogenate of the tissue of rat embryos at a concentration of 10-25 mg/ml, then after 15 minutes of observation in the upper part of the cuvette one can see a thickening of the interference bands: their total number in the range of vision increases by 4-5, which indicates a change in the optical density of the solution.

This can be accounted for as follows. In the vial, in the solution, there are not only embryo's tissues, but also ions and large molecular fragments, which got into it during the mechanical preparation of the homogenates. Such molecular remnants can penetrate to the bottom of the cuvette through the mentioned small pores in the filter. This results in an increase in the refractive index of the solution and the shift of interference fringes.

In the next phase, we studied the influence of MW radiation on the solution. For 10 minutes the solutions of embryo tissue, protein and DNA was irradiated by MW radiation with the frequency $\nu = 58 - 62$ GHz and the power of 3 mW/cm^2.

After bringing the irradiated solution in contact with a solution through the membrane filter in the cuvette for 3 minutes, no motion of bands happened. But then they started to move and after 15 minutes of observation,

Regular Paper

the interference pattern shift reached 4 bands. Experiments with biological macromolecules – proteins and nucleic acids – led to the following results. When a solution of bovine albumin is poured into the vial, then after 15 minutes the interference pattern is shifted by only 1 band or less. When we irradiated the solution of the protein in vitro for 10 minutes, no changes in the lower part of the cell were observed.

A different pattern of change was observed in the case of a solution with DNA molecules: after 15 minutes the shift of interference fringes was only about 0.7-1 bands. However, a 10-minute irradiation of the solution of DNA by MW irradiation resulted in a shift of 4 bands of the interference pattern already after 1-2 minutes; to the 15th minute of observation the shift reached 6.5 (Figure 2). Figure 3 depicts the changes that took

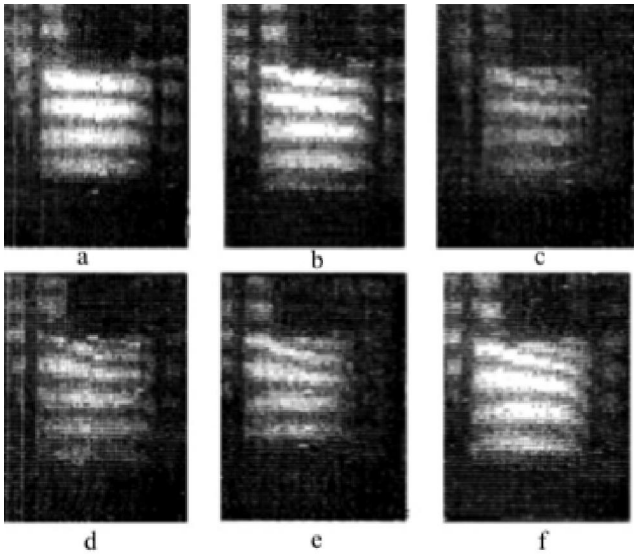

Figure 2 : Interference patterns of water solution of DNA molecules. A, b, and c – step-by-step low changes of the interference pattern of the solution that was not irradiated by MW; d, e, and f – are the visualization of significant changes in the solution affected by MW for 10 min.: d – 2 min. After irradiation, e – 10 min. After irradiation, f – 15 min. After irradiation.

place in the refractive index of the aqueous solution with DNA.

As is known, in aqueous solutions molecules of DNA form a kind of a gel around themselves – a large solvate shell, or "coat", of ions and molecular structures. MW irradiation may contribute to the separation of the "coat" from DNA and the percolation of the "coat's" components through the filter. It should be noted that in experiments with a mixture of proteins and nucleic acids we observed the same pattern, as was the case for the protein.

The interaction of ions, molecules and cells with surrounding tissues forms a "coat" around these entities, such that they cannot seep through the filter membrane. Exposure to MW radiation changes the interaction between cells as well as ions and molecules available in the solution. MW irradiation weakens the interaction and the molecular formations leave the "coat" while seeping into the lower solution, which is the cause of the observed shift of interference bands.

What is the mechanism of the influence of MW radiation on the solution of cells and biological molecules? Apparently, under the influence of MW radiation charge states on the cell surface change and due to the Coulomb interaction a "coat" of ions and molecular structures surrounds the cells. But maybe there is another type of the interaction, different from the Coulomb one, which is also holding the "coat"? Namely, it could be a quantum mechanical, or inerton interaction.

These examples do not answer the question of how MW radiation affects the charge state of the cells. It is unlikely that the electric field of MW radiation directly polarizes the cell membrane, since its intensity is low. In fact, by our estimate the strength is about 3 V/cm with intensity of 0.01 W/cm^2. However, such power may affect intracellular biochemical processes that lead to a

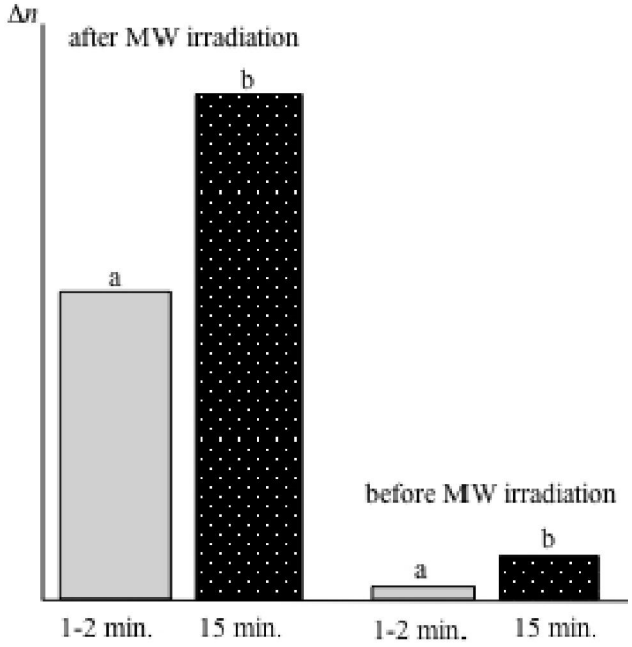

Figure 3 : Relative changes of the refraction index Δ*n* of an aqueous solution of DNA. A – the relative change of the refraction index after 1-2 minutes since the moment of first observation; b – the relative change of the refraction index after 15 minutes since the moment of first observation.

change of the charge state on the surface of cell membranes.

An example of intramolecular transformations under the action of MW radiation with a wavelength of 7.35 mm may be increasing the stability of the hemoglobin molecule to a transition from the active oxy-form into an inactive met-form. Without quanta of MW radiation a spontaneous detachment of an electron from the iron ion, which resulted in a redistribution of electric charges, is quite possible[13].

With the relaxation of states induced by the MW radiation field, the initial potential (charge) of cell membranes is recovered, which ultimately leads to the disappearance of the "coat". Experimentally, this manifests itself in the restoration of the movement and the interference fringes.

The above considerations are consistent with the experimental fact of a constantly changing dielectric constant under the influence of MW radiation. In addition, they allow us to explain the result of paper[14] in which the authors studied how MW radiation affected the erythrocyte sedimentation rate of healthy people and people with oncological brain diseases. It was found that 10-minute MW irradiation of blood with a frequency of 57.5 GHz and a power of 0.06 W/cm^2 lead to a significant increase in the erythrocyte sedimentation rate in sick patients, which was not observed in healthy people. One reason for the observed effect may be a change of charges on the surface of red blood cells caused by MW radiation. In healthy people, the induced charge relaxed to the initial (normal) state owing to biochemical reactions in 3-4 minutes. However, these processes of relaxation were disrupted in the case of sick patients; in their case MW radiation induced charges that could be stored for a long time. Additional charges resulted in the formation of a "coat" of molecules and ions around red blood cells causing them to appear "heavier".

It should be noted that red blood cells of people with leukaemia do have a surface charge. It was shown in paper[15] that in a NaCl solution erythrocytes settle by the principle of close packing of spheres, i.e. hexagonal packing, which is not observed in the case of normal, healthy red blood cells. Such a structure is realised only when the forces of interaction between its elements have spherical symmetry and this is typical for the Coulomb interaction.

In addition, under the influence of MW radiation on aqueous solutions of biological molecules the picture is complicated by processes of structuring of water molecules. Therefore, the relatively long time (minutes) during which the observed changes induced by MW radiation take place not only characterises intracellular relaxation processes, but also the relaxation processes occurring in the intra- and intermolecular interactions in a complicated system of water, oxygen, and biological molecules.

Samples of blood plasma water solution

Studies of the behaviour of a blood plasma water solution affected by MW radiation were also carried out. The most important changes due to MW radiation of a 2% blood plasma water solution was detected at 51.5 GHz frequency (Figure 4). When the MW source was switched on, a distance increase between object bands occurred. The changes in the interference picture were irregular with time. The largest changes occurred during the first minute, then slowed. Within the first 10 seconds the increase ranged up to half of the interference line and within 30 seconds, it ranged up to a full band. Without MW action, the number of interference bands was the same in the field of the object and around it and was equal to five. During 6.5 minutes from the start of exposure, the number of interference bands in the object's profile decreased by four. After this period, only slight changes were observed. Since these changes were observed in the whole plasma volume, their nature was regarded as being macroscopic. Changes in the refractive index of the sample under MW action were estimated by expression (1).

We could see the reversibility of the effect: after the MW source was switched off, the interferogram restored its original structure; the relaxation period to the original state was 3-4 minutes longer than the time it took to achieve maximum change. The increase in plasma concentration up to 10% essentially slowed the process of changes, whereas the addition of 1.5% of $CaCl_2$ into the solution increased the rate of the interference image shift more than twofold. Experiments showed that a seven minute MW radiation action on pure water carried our at 41.5 GHz frequency resulted only in minor changes of the interference image, though a 5 minute exposure at 51.5 GHz frequency decreased the number of interference bands by one.

Regular Paper

Thus, weak MW-field effects also occurred in water, though their magnitude was small ($\Delta n = 2 \times 10^{-5}$). These facts suggest that the effect is mainly determined by the blood plasma components. MW irradiation and heating effects were oppositely directed. Temperature rise in the flask detected by a thermosensor during the MW action with a power density of 10 mW/cm^2 amounted to 0.5-0.6 K. The estimation of the temperature effect by using the thermal conductivity equation and thermal balance equations showed that the maximum possible heating of the solution during this time could amount to 1 K. The calculation showed that even in the absence of heat exchange between the solution and the environment under the radiation effect with a power density of 10 mW/cm^2, the temperature of the solution with a volume of 1.5 cm^3 could raise about 1 K within 6 min. A lower temperature value (0.5-0.6 K) was obtained in measurements using the thermosensor. The temperature coefficient of changes in the refraction index of water is 6×10^{-5} K^{-1}. In our experiment the maximum change of the refraction index reached $n = 2.59 \times 10^{-4}$, which is an order higher than the effect of temperature change on the refractive index. Taking both effects into account, the cumulative effect results in about $n = 3 \times 10^{-4}$.

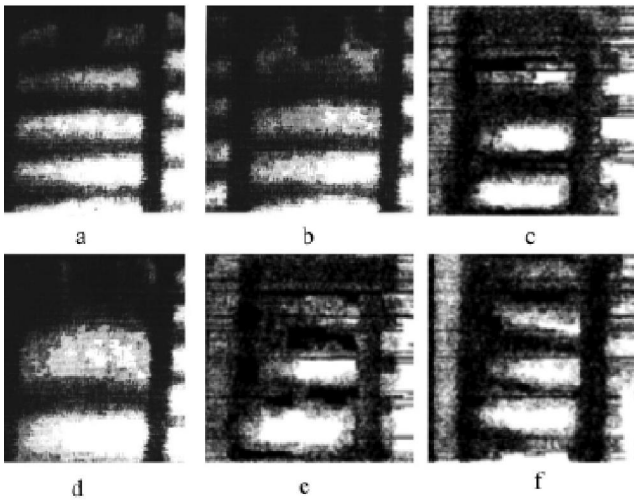

Figure 4 : Interference patterns of the 2% plasma solution under the action of MW irradiation at ν = 51.56 ghz: at the beginning of irradiation: a – 10 s, b – 30 s, c – 5 min., d – 6.5 min.; after switching off the MW: e – 5 min, f – 13 min.

The experimental data and numerical estimate demonstrate that the changes in refraction under MW action were conditioned by non-thermal changes of the dielectric constant of the solution, which can be described as a sum of contributions of electronic, vibration and orientation components. It is known that at room temperature water molecules create a continuous net structure formed by hydrogen bonds fluctuating in time. In solutions, the structure includes hydrate shell clusters whose dimensions depend on the charges and sizes of hydrated molecules or ions, and temperature. Considering that about 10^{11} translational and orientation motions occur per second in pure water, an external electromagnetic field at this frequency is likely to perform a resonance orientation effect upon the hydrogen bond net structure. Evidently, structural rearrangements took place in the plasma solution and in its components – biomolecules and water molecules, which in turn affect the dielectric constant of the solution. Besides, in water solution containing blood plasma macromolecules (albumin, globulin etc.) another possibility of macromolecule coherent resonance vibrations in water molecule environment emerges. This possibility is connected with the probable manifestation of cooperative effects with the participation of large groups of macromolecules under weak energy impulses of a resonance frequency electromagnetic field. Thus, low-energy MW radiation initiates processes of internal rearrangements in bio macromolecules, which can result in a modification of the electronic polarizability that contributes to the observed total change of the refraction index.

By using the holographic interferometer we can visualize and test the interaction between different tissues. An interference pattern allows us to study the interaction of cell products with tissues in a water solution in cuvette "8" (Figure 1). Studying of the number of bands and sign of the changes in the interference patterns, we can observe the dynamics of products of metabolism from upper cuvette "7" with tissues or cells in lower cuvette "8". The characteristics of interference patterns were changed essentially when a solution with tissue underwent a radiation with MW. From the experiments we can conclude that the tissue interaction drastically changes under MW action. This state is maintained for some period of time (3-5 minutes) and then it relaxes to its original state. The hypothesis of charge changes of cells and their components under MW radiation seems consistent.

Inerton field effects

The notion of an inerton field was introduced theoretically in papers[16-21] and then proved experimentally in a number of works[10-12,22-24]. Inertons are quasi-particles, which represent field particles of the field of inertia[16,17]. Inertons form a cloud around any moving quantum particle, such as electron, proton, atom, etc. In the real physical space a particle is characterised by its kernel (central particle) and a cloud of inertons; in an abstract phase space such system of the particle and its cloud of inertons is described by the well-known quantum mechanical ψ-wave function. During fast processes a particle may loose part of its inertons from the particle's inerton cloud. Thee free inertons are able to influence other systems changing their chemical physical properties, first of all, such as the strength of the interaction between particles.

A Teslar watch is one of the applications of inerton fields. The Teslar watch includes a special chip, a Teslar chip – a ferromagnetic strip folded and sealed, which is a typical Möbius strip. The strip is induced with a signal of about 8 Hz. In the presence of the electromagnetic field generated by the watch's mechanism, the Möbius strip starts to react to the signal and compensates magnetic components. In the process, its inerton component is generated. The Teslar chip is able to locally influence chemical physical processes. In our works[10-13] we performed detailed studies of the influence of the Teslar chip on different chemical physical systems.

As the model of primary reception able to react to an external inerton field we chose the following systems: (i) saturated aqueous solution of amino acids (tyrosine, tryptophan, and alanine); (ii) diluted aqueous solution of human blood plasma (in the case of blood plasma biomolecules, the system in question was non-equilibrium and even very small stimuli applied to it could be effective.)

The Teslar chip was put onto the top of a quartz cuvette with the size $1 \times 1 \times 4.3$ cm^3 filled with the solution studied (the Teslar chip was put at the position "7", Figure 1). If the dielectric characteristics of the object studied are the same before and after the Teslar chip influence, the fringe pattern remains unaltered and interference bands inside and outside the object's profile continue each other. However, if an external factor causes changes of n, the fringe pattern within the limits of the object's profile will change. Aqueous solutions were prepared on the basis of pure bidistilled water. Prepared solutions, before the experiment, were maintained for 24 hours under 25 °C. The plasma blood solution was extracted from the blood of a patient with a heart vascular disorder just after the blood was drawn at a hospital by conventional methods. We dilute the solution with distilled water at ratios of 1 : 50 and 1 : 100. The time between the blood extraction and the holographic measurement was 4 hours. The procedure of dynamic measurement consisted of a sequence of records of interference patterns on a special thermoplastic plate, which was then recorded by a digital video camera. Afterward, the images were entered into the computer and evaluated. For determination of the interference band centre, 10 points along the horizontal line of the cuvette have been chosen.

The studies were conducted at a temperature of 20 $\pm$ 1.5 °C. The most important constraint in the experiment was to protect the cuvette from the temperature gradient and the airflow. The latter two disturbance factors can result in an inner instability of the system. In Figure 5 (left), typical interference patterns of the aerial ambient space and the aqueous solution are presented. Vertical black lines show the image of the cuvette corner (its size is $1 \times 1 \times 4.3$ cm^3). Thus, in our experiments we have been able to observe an alteration of the reflective index in the surface zone of the cuvette equal to 1×2 cm^2 that is determined by the cuvette size and the aperture of the laser beam. In Figure 5 (left), typical interference patterns of the aerial ambient space (Air) and the aqueous solution (Solution) are presented. Vertical black lines show the image of the cuvette corner (its size is $1 \times 1 \times 4.3$ cm^3). We were able to observe an alteration of n in the surface zone 1×2 cm^2 of the cuvette (the cuvette size) and the aperture of the laser beam. Deformations of the interference pattern in different points of the solution have been caused by changes in n in these points.

The resolution is defined by the location of the optical wedge, namely, by a sum of horizontal interference lines. The space resolution is about 2 mm. The method described gives the possibility to follow the response of the solution with the time factor of minimal discontinuous ability equal to 10 seconds. A sequence of pictures of the fringe pattern characterizes the space dynamics of the system studied in any place of the cuvette. For example, Figure 6 (b) shows the fringe pattern formed

Regular Paper

after about 4 minutes starting from the moment of ac-

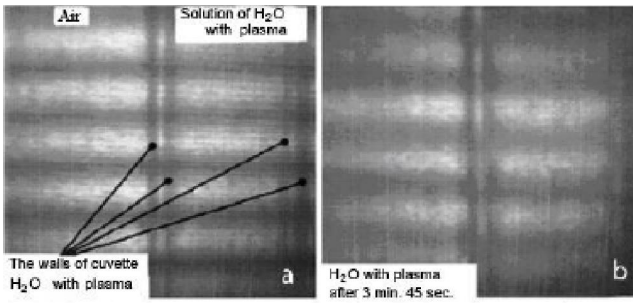

Figure 5 : Dynamics of the fringe pattern of the aqueous solution of human blood plasma without the influence of the Teslar chip. The value of the effect is estimated by the difference between the shift of the interference band in the cuvette with the solution and the position of the same band in the air; we evaluated the shift of interference bands before and after the Teslar chip application. It is seen that after 4 minutes the bands in the cuvette were not deformed and were essentially not moved relative to those in the air.

tion of the Teslar chip that was positioned 2 mm from the cuvette. Changes of interference bands that occurred during this time are associated with an internal stimulus.

A series of experiments was conducted with distilled water, the saturated aqueous solution of L-tyrosine and β-alanine respectively at 25 °C. The results showed typical slight changes of the fringe pattern after a 400 seconds or larger time interval. These changes should be associated with the inner drift of the liquid parameters. The curve of long-time dynamics does not show any influence on the side where the Teslar chip is located, close the cuvette. The other behaviour and picture have been observed in the case of the blood plasma solution. Without the Teslar chip action, this solution showed stable and reproducible characteristics during more than 4 hours.

During more than one hour, the recorded system and the objects of study (the solution of plasma and water) were stable and reproducible. In Figure 6, we present the image of the cuvette with blood plasma solution affected by the Teslar chip. Black dots indicate the centre position of one of the interference bands on the image plane. The value of the shift relating to the zero line characterizes the degree of influence of the Teslar chip. Black rectangles (Figure 6, right) show the positions of two Teslar chip's in relation to the cuvette; the fringe pattern of the solution relating to the chip is deformed in different ways in different zones (short, mid, and far-distance). The physical mechanism of the change is associated with the increase of n in the short-dis-

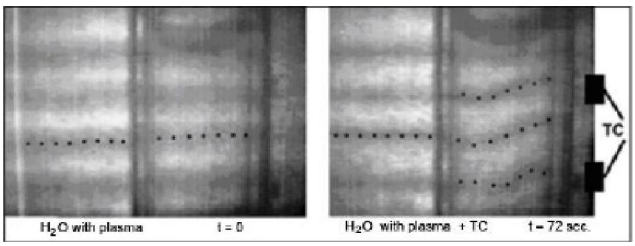

Figure 6 : Dynamics of the fringe pattern of the aqueous solution of human blood plasma after the insertion of 2 Teslar chips (TC in the Figure). The strong disturbance of the optical density of the solution emerges already after 72 s, right figure. (The back covers of two sections of the bracelet are found at 4mm from the right wall of the cuvette).

tance zone; n remains unchanged in the mid-distance zone and decreases in the far-distance zone.

Moreover, it seems that slow laminar flows were induced by the Teslar chip near the front wall and directed to it. If the refraction index of the solution changes in one place under the influence of an external factor, the length of the optical path will also change. With the purpose of the registration of the changes, the device is designed in such a way that the "starting interferogram" constitutes a family of horizontal bands of equal thickness. Depending on the character of changes of the optical density in the cuvette volume, the bands can be distorted (local changes of n), gaps between bands can expand without deformations (decrease of n in part of the volume). Arbitrary deformations of the fringe pattern are caused by a combination of local and global changes of the optical density. Changes of n are produced by changes in the structure of the network of hydrogen bonds of water, which under the influence of oxygen, biomolecules and the inerton field generated by the Teslar chip, forms long-lived structures. In the mentioned network, those new structures try to minimize the total energy relative to the volume occupied by the water system. Such kinds of changes (structuring of the aqueous solution) occur sufficiently slowly and therefore allow the recording by optical methods. The strongest changes in effects associated with the Teslar chip were detected during the first 5 to 15 minutes starting from the moment of influence. The saturation effect was reached after 10 minutes. Without the Teslar chip, the number of interference bands remained the same in the field of the object and around it and was equal to five. Changes in the refractive index n of the sample affected by the Teslar chip are estimated from eq. (1).

Influence of the Teslar chip on water leads only to minor changes of the fringe pattern, $\Delta n = 2 \times 10^{-5}$. The behaviour of proteins is mainly determined by the influence of the Teslar chip. The maximum change of *n* of the protein solution affected by the Teslar chip reached the value of $\Delta n = 2 \times 10^{-4}$, which is an order of magnitude larger than the temperature induced changes of *n*.

A specific feature of the Teslar chip's influence consists in the fact that the inerton field effect is still preserved after removing the Teslar chip (the memory effect that is characteristic of different water systems). In Figures 7 and 8 one can see fringe patterns of water and the aqueous solution, respectively, after their destruction. Here, the destruction means a mechanical stir of the liquid sample with a syringe. This procedure consists in extraction of a portion of the liquid sample from the cuvette and the subsequent filling of the cuvette again (without any gas bubble formation) with the extracted

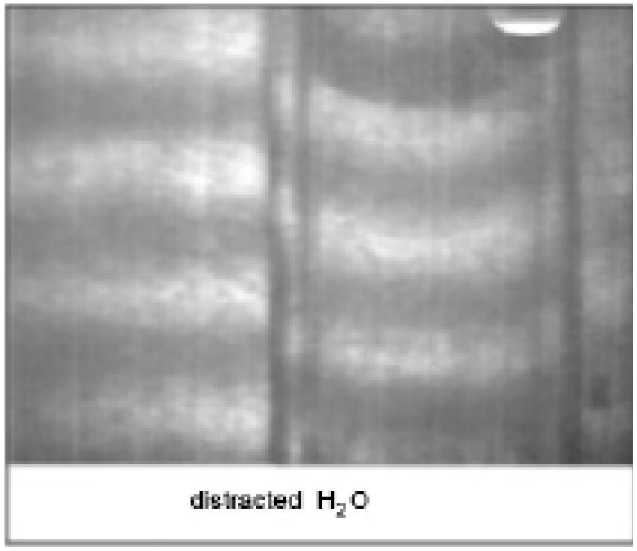

Figure 7 : The fringe pattern of the cuvette with distilled water after an intensive mechanical action (a turbulent action in the liquid with a syringe with a thin needle as described above).

liquid; the procedure was done twice.

15 minutes after the second re-filling of the cuvette, the fringe pattern was recorded. We show that both distilled water (Figure 7) and the aqueous solution of blood plasma (Figure 8) show very similar responses to this procedure. However, in the case of the aqueous solution of plasma previously affected by the Teslar chip, the solution is specified by the turbulent-like picture, Figure 8 (right).

In Figure 9, experimental dots show changes of *n* of the solution (the vertical axis) at the cuvette's back wall against the upper Teslar chip (rectangles) and the lower Teslar chip (triangles); recall the two chip are located near the front wall (see Figure 7). Current time, in seconds, is plotted along the horizontal axis. Legends "H_2O" (the blue background) and "H_2O with plasma" (the orange background) indicate different solutions in the cuvette. Time intervals are singled out for: (1) the magnet ("Magnet" on the green background) was applied to the front wall of the cuvette and (2) two links of the bracelet with two Teslar chips were set into the cuvette (the violet background). Moments of intermix of the solution (Destruction) are shown by means of arrows; the intermix was made by using a medical syringe with 0.2 mm needle; the solution was absorbed from the cu-

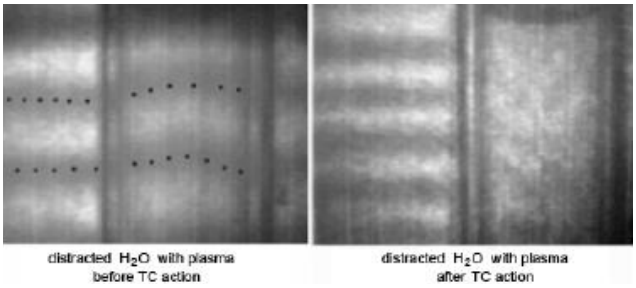

Figure 8 : Comparative picture of the plasma solution response to a turbulent action with a syringe depending on the prehistory of the sample. The left picture shows the response of the solution before the influence of the Teslar chip; the right picture is the same solution after the 15-minute irradiation by 2 Teslar chip.

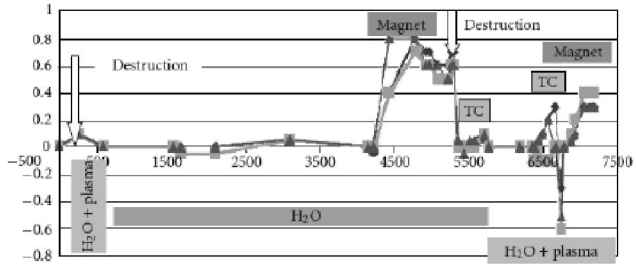

Figure 9 : Dynamics of changes of the fringe pattern of the cuvette's volume at different external factors. The vertical axis show relative changes of the refractive index. The horizontal axis shows current time in seconds.

vette by the syringe and then poured back, twice.

The insertion of the magnetic field induced a response on the side of pure distillated water in the cuvette, because the water had dissolved oxygen (oxygen is a strong paramagnetic); some more details on the behaviour of the refraction index is shown in Figure 10. After the destruction described above, we inserted the two links of bracelet with two Teslar chips into the system studied

Regular Paper

(see Figure 6). However, the availability of two Teslar chip does not produce any response from the water. Then the same experiment was carried out on the plasma solution. In this case the solution gave a response. Deformations of the fringe pattern indicate that the refraction index decreases on the opposite wall of the cuvette. If in this case we replace the two Teslar chips by a magnet, deformations of the fringe pattern become opposite, which means that the refraction index increases.

Changes in the aqueous solutions cover the entire macroscopic volume; the system affected by the Teslar chip reacted as a whole. This can be associated with both inner convective flows (as with Bénard cells) and structural changes of water. Under the water structure we mean the space architecture of domains arising under a spontaneous separation of the liquid and the redistribution of hydrogen bonds. The latter could lead to changes in both the reflective index of the solution and the fringe pattern.

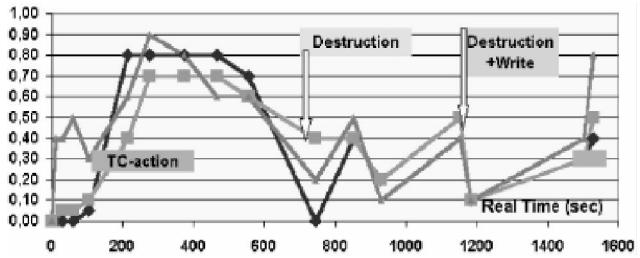

Figure 10 : The chart shows more detailed dynamics of the plasma solution in the upper part of the cuvette (just against the upper TC) near the back wall [rectangles], in the centre of the cuvette [triangles] and near the front wall of the cuvette [black rhombus]. The vertical axis shows relative changes in the refractive index. The horizontal axis shows current time in seconds.

CONCLUSION

By using the holographic interferometer we could observe the behaviour of bioorganic solutions and their response to low-energy MW radiation as well as low frequency inerton radiation. The method of interferometry allows us to reveal subtle effects not revealed in other optical studies. In particular, we observed specific dynamics in the bioorganic systems launched by both MW and inerton radiation. These two fields initiate processes of internal rearrangements in biomacromolecules.

In the case of MW radiation, it induces an electronic polarizability of biomolecules contributing to the observed total change of the refraction index. The polarization mechanism changes the conformation state of long biomolecules, which gives rise to the rearrangement of these molecules[25].

In the case of a low-energy and low frequency inerton field the rearrangement of molecules is stipulated by an additional weighting of molecules that absorb inertons, which tends to shift the molecules' equilibrium positions[20].

Inerton fields transfer mass, changing potential properties of the environment. Consequently, the mass defect Δm becomes an inherent property not only of atomic nuclei but also of any physical, physical chemical, and biophysical systems[14]. Besides, an inerton field also transfers fractal properties of matter and it seems that this field may be responsible for such phenomena as homeopathy and the effects of informational medicine.

ACKNOWLEDGEMENT

The authors thank greatly the late Prof. M. P. Lisitsa and the late Prof. L. I. Berezhinsky for the useful discussions and the amendments to the text of this work.

REFERENCES

[1] H.Frohlich; Biological coherence and response to external stimuli, Springer-Verlag, Berlin, Heidelberg, New York, London, Paris, Tokyo, **(1988)**.

[2] E.S.Ismailov; Biophysical action of high frequency. Fundamental and applied aspects of millimetre electromagnetic field in biology and medicine, in Proceedings of I Symposium with International Participants, Kyiv, Soviet of Ministry of Ukraine, Temporal Scientific Centre "Vidhuk", **(1989)**.

[3] H.Chengjiong, G.Kehui, H.Gunzhu; Effects of microwave acupuncture on the immunological functional cancer patients, Journal of Traditional Chinese Medicine, **7**, 9-11 **(1987)**.

[4] A.A.Serikov; Weak field influence on biomolecular changes, Journal of Biological Physics, **18**, 65-77 **(1991)**.

[5] I.Ya.Belyaev, Y.D.Alipov, V.S.Shcheglov; Chromosome DNA as a target of resonant interaction between E. coli cells and low-intensity millimetre waves, Electro and Magnetobiology**, 11(2)**, 97-108 **(1992)**.

[6] G.S.Litvinov; Response of biomolecules and cells to millimetre wave electromagnetic field. Transactions of the First Congress of European Bioelectromagnetics Association, in Vth European Symposium, Brussels, Belgium, 46 **(1992)**.

[7] G.S.Litvinov, L.I.Berezhinsky, G.I.Dovbeshko, M.P.Lisitsa; Mm-wave radiation action on infrared reflection spectra β-alanine single crystal, Biopolimery i kletka, (in Russian), **3**, 77-82 **(1991)**.

[8] G.Dovbeshko, L.Berezhinsky, V.Obuchovsky; Special case of nonlinearity of biological molecules, Proceedings of SPIE, **2795**, 306-311 **(1996)**.

[9] L.I.Berezhinsky, N.Ya.Gridina, G.I.Dovbeshko, M.P.Lisitsa; Visual observation of mm- wave action upon blood plasma, Biophysics, (in Russian) **38(2)**, 378-384 **(1993)**.

[10] E.Andreev, G.Dovbeshko, V.Krasnoholovets, The study of influence of the Teslar technology on aqueous solution of some biomolecules, Research Letters in Physical Chemistry Article ID 94286, **2007**, 5.

[11] V.Krasnoholovets, S.Skliarenko, O.Strokach; On the behaviour of physical parameters of aqueous solutions affected by the inerton field of Teslar technology, International Journal of Modern Physics B, **20(1)**, 111–124 **(2006)**.

[12] V.Krasnoholovets, S.Sklyarenko, O.Strokach; The study of the influence of a scalar physical field on aqueous solutions in a critical range, Journal of Molecular Liquids, **127(1–3)**, 50–52 **(2006)**.

[13] V.I.Gaiduk, Yu.I.Khurgin, V.A.Kudryashova; Outlook for study of the mechanisms of the nonthermal effects of millimetre-and submillimetre-band electromagnetic radiation on biologically active compounds, Soviet Physics Uspekhi, (in Russian), **16(3)**, 577–578 **(1974)**.

[14] G.S.Litvinov, N.Ya.Gridina, L.I.Matseiko; Low intensity mm-wave influence on the erythrocyte sedimentation rate, The SPIE int. conf. on millimetre and submillimetre waves and applications, San Diego, California, Jan 10-14, 1994; SPIE, **2250**, 303-307 **(1994)**.

[15] B.N.Basov, M.B.Golovanov; The method of calculating the degree of periodicity of the arrangement of leukemic cells in suspension, Biofizika, (in Russian), **36(1)**, 114-116 **(1991)**.

[16] V.Krasnoholovets, D.Ivanovsky; Motion of a particle and the vacuum, Physics Essays, **6(4)**, 554-563 **(1993)**.

[17] V.Krasnoholovets; Motion of a relativistic particle and the vacuum, Physics Essays, **10(3)**, 407-416 **(1997)**.

[18] V.Krasnoholovets; Submicroscopic deterministic quantum mechanics, International Journal of Computing Anticipatory Systems, **11**, 164–179 **(2002)**.

[19] V.Krasnoholovets; On the origin of conceptual difficulties of quantum mechanics, In: *Edition* F.Columbus, V.Krasnoholovets 'Developments in Quantum Physics', Nova Science, New York, USA, 85-109 **(2004)**.

[20] V.Krasnoholovets; Variation in mass of entities in condensed media, Applied Phyics Research, http://www.ccsenet.org/journal/index.php/apr/article/view/4287, **2(1)**, 46-59 **(2010)**.

[21] V.Krasnoholovets; Reasons for the gravitational mass and the problem of quantum gravity, *Edition* M.Duffy, J.Levy, V.Krasnoholovets 'Ether space-time and cosmology, Modern ether concepts, relativity and geometry', PD Publications, Liverpool, **1**, 419-450 **(2008)**.

[22] V.Krasnoholovets, V.Byckov; Real inertons against hypothetical gravitons. Experimental proof of the existence of inertons. Indian Journal of Theoretical Physics, **48(1)**, 1-23 **(2000)**.

[23] V.Krasnoholovets, N.Kukhtarev, T.Kukhtareva; Heavy electrons: Electron droplets generated by photogalvanic and pyroelectric effects, International Journal of Modern Physics B, **20(16)**, 2323-2337 **(2006)**.

[24] V.Krasnoholovets; Sub microscopic description of the diffraction phenomenon, Nonlinear Optics Quantum Optics, **41(4)**, 273–286 **(2010)**.

[25] L.L.Berezhinsky, N.Ya.Gridina, G.I.Dovbeshko, M.P.Lisitsa, G.S.Litvinov; Action of millimetre radiation on the blood plasma, Biofizika, (in Russian), **38(2)**, 378-384 **(1993)**.